Technical Sciences, 2024, 27, 33–53

UNIWERSYTET WARMIŃSKO-MAZURSKI W OLSZTYNIE

Yearbook peer-reviewed scientific journal

ISSN 1505-4675
e-ISSN 2083-4527

TECHNICAL SCIENCES

Homepage: https://czasopisma.uwm.edu.pl/index.php/ts/

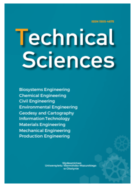

DOI: https://doi.org/10.31648/ts.9545

APPLICATION OF TRANSITION FINITE ELEMENTS IN *hpq*-ADAPTIVE MODELING AND ANALYSIS OF MACHINE ELEMENTS

Magdalena Zielińska[1], ***Grzegorz Zboiński***[2]

[1] ORCID: 0000-0002-8702-6558
Department of Mechanics and Basics of Machine Design
Faculty of Technical Sciences
University of Warmia and Mazury in Olsztyn
[2] ORCID: 0000-0001-7775-2436
Department of Mechanics and Basics of Machine Design
Faculty of Technical Sciences
University of Warmia and Mazury in Olsztyn
Institute of Fluid Flow Machinery
Polish Academy of Sciences in Gdańsk

Received 29 October 2023, accepted 11 March 2024, available online 11 March 2024.

Keywords: finite element method, adaptivity, transition models, modeling, analysis, machine elements.

Abstract

This paper concerns the modeling and analysis of machine elements using the adaptive finite element method. The adaptation used is of *hpq* type, which means that the finite element dimension h and element transverse q and longitudinal p approximation order may be different in each element. These parameters are determined automatically by the program to obtain modeling and approximation error levels not higher than the assumed admissible level of the errors. The presented paper focuses on the use of transition elements between basic elements corresponding to the three-dimensional theory of elasticity and the first-order shell model. Three applied transition elements differ in their assumptions regarding the continuity of the displacement, strain, and stress fields between the basic models. The effectiveness of the application of transition elements was assessed in terms of the removal of the internal boundary layer at the boundary between the models and the convergence of adaptive solutions taking into account these models.

Correspondence: Magdalena Zielińska, Katedra Mechaniki i Podstaw Konstrukcji Maszyn, Wydział Nauk Technicznych, Uniwersytet Warmińsko-Mazurski, ul. Oczapowskiego 11, 10-710 Olsztyn, e-mail: m.nosarzewska@uwm.edu.pl

Introduction

Three aspects will be presented in this introduction briefly. We will start with the research motivation, then the available literature will be mentioned and finally novelty of the paper will be determined.

The motivation for the research

Strength calculations within CAD (computer-aided design) are most often performed using commercial FEM (finite element method) codes. Such codes are assigned primarily to the analysis of structures and machine elements (parts) described by one mechanical model. These codes generally have a developed library of finite elements corresponding to such models. These programs cope very well with the analysis of individual structural elements and individual machine parts. However, these programs fail when different functional parts are joined together, e.g. plates and shells with solids. The second weakness of modern CAD systems used for the numerical analysis of machine parts is the classical nature of the finite element methods used. The solution is performed once, on a pre-defined mesh of finite elements. This classical approach does not allow for determining the error level of the solution or for reducing it automatically in areas where the error is too large. Removing both of the above-mentioned disadvantages of the classical approach requires the use of an adaptive finite element method, in which the solution is performed many times and the mesh is rebuilt based on the error level.

In modern elastic analysis of complex structures, including thin-walled, thick-walled, and bulky (three-dimensional) parts, there is a tendency to use different mechanical models in these different parts. These are generally basic models described by known mechanical theories. The common application of such models can be implemented in three ways. The first way is to introduce constraints at the boundaries of these models. This involves leaving the degrees of freedom available in both models as active and blocking those that are specific to one of the models. The second way is to introduce transition models, which means that the unknown field in one part of the element corresponds to the first basic model and in the remaining part to the second basic model. The third way is to use the same basic model in all parts of the complex structure.

The disadvantage of the first method is that the constraints at the model boundaries result in the appearance of an internal boundary layer or singularities at this boundary. The second approach requires the similarity of the basic models used for the creation of a transition model. Such similarity is not always the case. In turn, the third approach does not solve the problem of combining basic models but rather circumvents it.

State-of-the-art issues

Analyzing the related literature in terms of the availability of CAD systems for adaptive analysis of complex elastic structures, it can be noted that existing programs for numerical calculations based on FEM should be supplemented with *hp*-type adaptation options, where *h* and *p* represent element dimension and approximation order, respectively. This would guarantee a higher (exponential) order of convergence than is present in some FEM codes using *h*-type adaptation (with an algebraic order of convergence). In turn, model adaptation, which is not available in CAD programs at all, requires, in the field of solid mechanics, the introduction of adaptive transition elements, including those used to connect three-dimensional and shell models. Due to the vast amount of available literature on all the above-mentioned issues, we will limit our survey to examples that correspond to the adaptive analysis of complex elastic structures. These are structures composed of solid, thick- and thin-walled and transition parts. We will be mainly interested in the three-dimensional formulation, which uses only three-dimensional degrees of freedom in all parts of the complex structures. The transition elements available in the literature are largely classical, which does not enable their use for adaptive analysis of complex structures (COFER, WILL 1991, DÁVILA 1994, GMÜR, SCHORDERET 1993, RANK, BUŠKA 1987, SURANA 1980, 1982, 1983, 1987). On the other hand, adaptive transition elements are available (GUPTA 1978, HUANG, XIE 2011, JEYACHANDRABOSE, KIRKHOPE 1984, WAN 2004). All of them are characterized by a fixed three-dimensional state of strains and stresses in transition zones. This results in high stress and strain gradients between the basic models at the interface. These gradients, in turn, result in the deterioration of solution convergence when transition models and elements are used for complex structure modeling and analysis.

Novelty and scope of the paper

Our previous works on the use of transition models concerned simple model structures (plates and shells). In this work, we will demonstrate that these models can also be used for modeling and analysis of real objects found in technology. We will do this using adaptive modeling and *hpq*-adaptive finite element analysis. In this method, *h* is the dimension of a finite element, while *p* and *q* are the longitudinal and transverse orders of approximation in the element. Let us note that the order *q* is the order of the hierarchical model used to describe the shell and transition parts of complex structures. Our hierarchical models and *hpq*-adaptive hierarchical approximations have been described in ZBOIŃSKI (2001, 2010) and are motivated by works of ODEN and CHO (1996), SZABÓ and SAHRMANN (1988), SCHWAB (1998), DEMKOWICZ (2006). Shape functions applied in these approximations are presented in ZBOIŃSKI and JASIŃSKI (2007), ZBOIŃSKI and OSTACHOWICZ (2001), ZBOIŃSKI (2001) for shell, solid-to-shell transition, and three-dimensional models, respectively.

The basic models of the three-dimensional theory of elasticity (and higher--order shell theories as well) are characterized by a three-dimensional state of stress and strain. On the contrary, in the first-order shell theory – plane stress state and kinematic assumptions (deformation of straight lines normal to the mid-surface into straight lines and no extension of these lines) hold. The difference in the stress and strain states in the basic models makes it necessary to introduce a transition model. The classical model guarantees continuity of displacements at the common boundary of the three-dimensional model and the first-order shell model. The modified transition model additionally delivers a transition stress state from three-dimensional to plain in the transition region. Finally, the enhanced model additionally ensures a continuous change in the kinematic assumptions of the first-order theory from the absence to the validity of these assumptions between the three-dimensional model and the first-order model. In this paper, we will compare three transition models in the context of their application to technical complex objects.

The applied transition models and elements

The transition elements considered in this paper are of a solid-shell or hierarchical-shell nature. The first type of element is used to combine elements of the three-dimensional theory of elasticity with first-order shell elements. The second type is used to connect hierarchical shell elements with first-order shell elements. In both cases, the structure and algorithm of the transition element are the same.

The classical transition model used in numerical calculations makes it possible to combine elements described by the three-dimensional theory of elasticity and elements corresponding to the Reissner-Mindlin plate or Reissner shell theories. When using this type of transition model, continuity of deformation between the basic models is achieved, but with high gradients at the boundary between the transition and shell models. The classical transition model does not allow for stress continuity at this boundary. Details of the algorithm and numerical studies of this transition model are presented in the works (NOSARZEWSKA 2007, ZBOIŃSKI 2001).

Next, a modification of the transition model was proposed (ZIELIŃSKA, ZBOIŃSKI 2013). The modified model still guarantees the continuity of transverse deformations at the boundaries of the transition model, still with high gradients at the interface of the shell and transition models. The introduced changes allowed for continuity in the stress field thanks to the introduction of a correcting transition function into the computational algorithm (NOSARZEWSKA, ZBOIŃSKI 2009).

The last, most advanced transition model, introduced in ZIELIŃSKA and ZBOIŃSKI (2014a), still guarantees the continuity of the stress field at the interface of the combined models. Additionally, this model achieved a continuous change in the kinematic assumptions of the Reissner-Mindlin theory in the transition zone (ZIELIŃSKA, ZBOIŃSKI 2014b, p. 63-72).

Numerical analysis

The numerical analysis concerned the assessment of the ability of the transition elements to remove the internal boundary layer, as well as the assessment of the convergence of the adaptation process within the complex structure. The analyzed complex structure corresponded to the symmetrical half of the simplified model of a rotating machine blade (Fig. 1). We used the simplified geometrical representation of the blade, however, also the curved geometry of the blade could have been used. The structure was modeled using three types of finite elements: three-dimensional (blade base), shell (blade airfoil), and transition (airfoil-base connection). However, due to the qualitative and quantitative similarity of the results obtained for the models with the enhanced and modified transition elements, the results with the modified element were skipped. Thus, only the results obtained for the classical and enhanced transition element cases are presented.

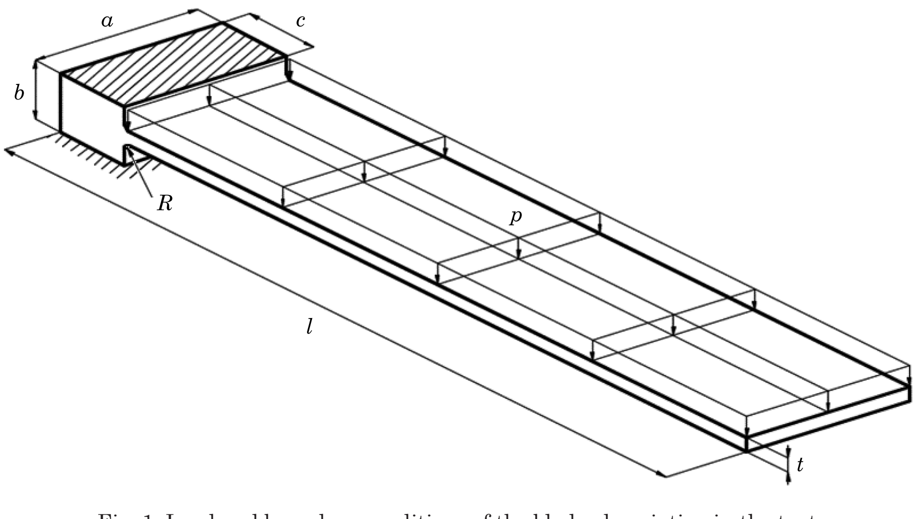

Fig. 1. Load and boundary conditions of the blade; description in the text

The length of the structure will be $l = 0.84$ m, while the width $a = 0.24$ m. The dimensions of the cuboid base will be $a \times b \times c – 0.24 \times 0.05 \times 0.06$ [m]. We will assume the thickness of the blade airfoil to be $t – 0.01$ m. The transition geometrical part connecting the airfoil with the base will be limited by a quarter of a circle with a radius of $R = 0.02$ m. The top and bottom surfaces of the base will be fixed. The load will be normal pressure applied to the upper surface of the blade. Its value will be $p = 1 \cdot 10^5$ N/m^2. We assume that the structure is made of an elastic material with Young's modulus $E = 2.1 \cdot 10^{11}$ N/m^2 and Poisson's ratio $v = 0.3$.

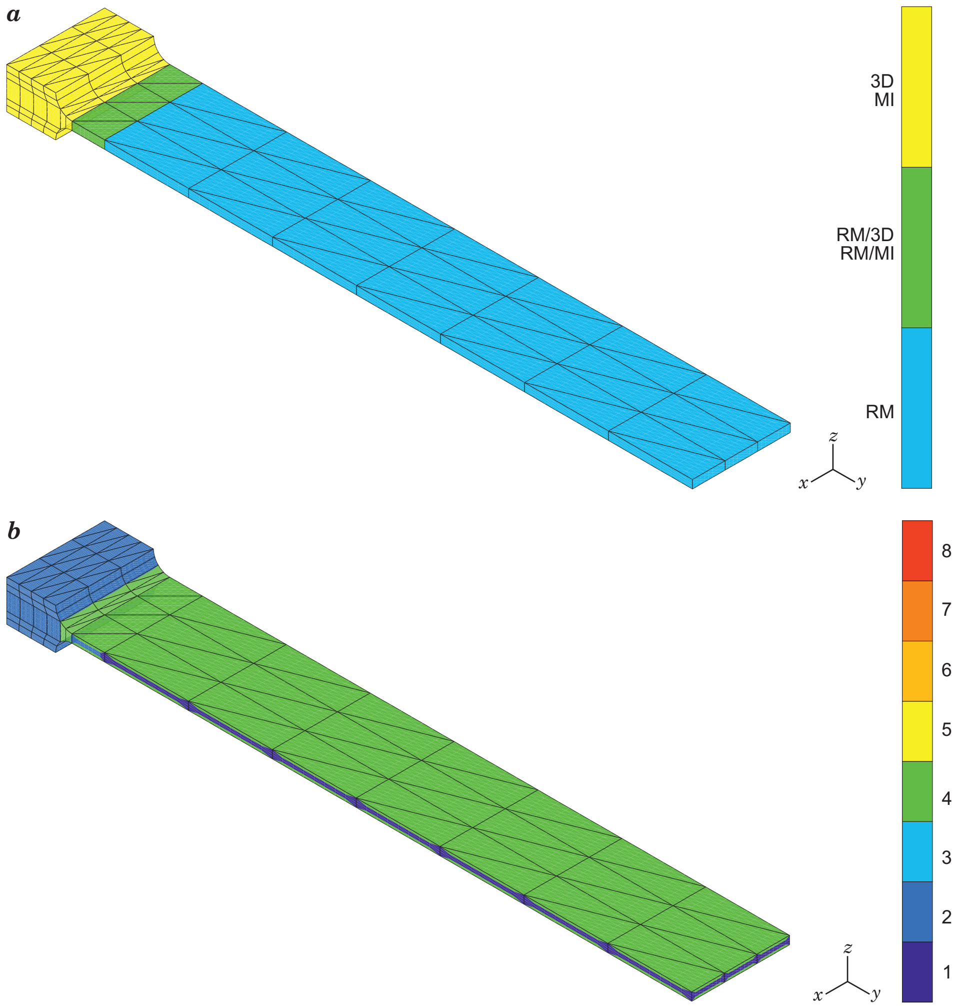

Fig. 2. Initial mesh with either classical or enhanced transition elements:
a – applied models, *b* – approximation orders

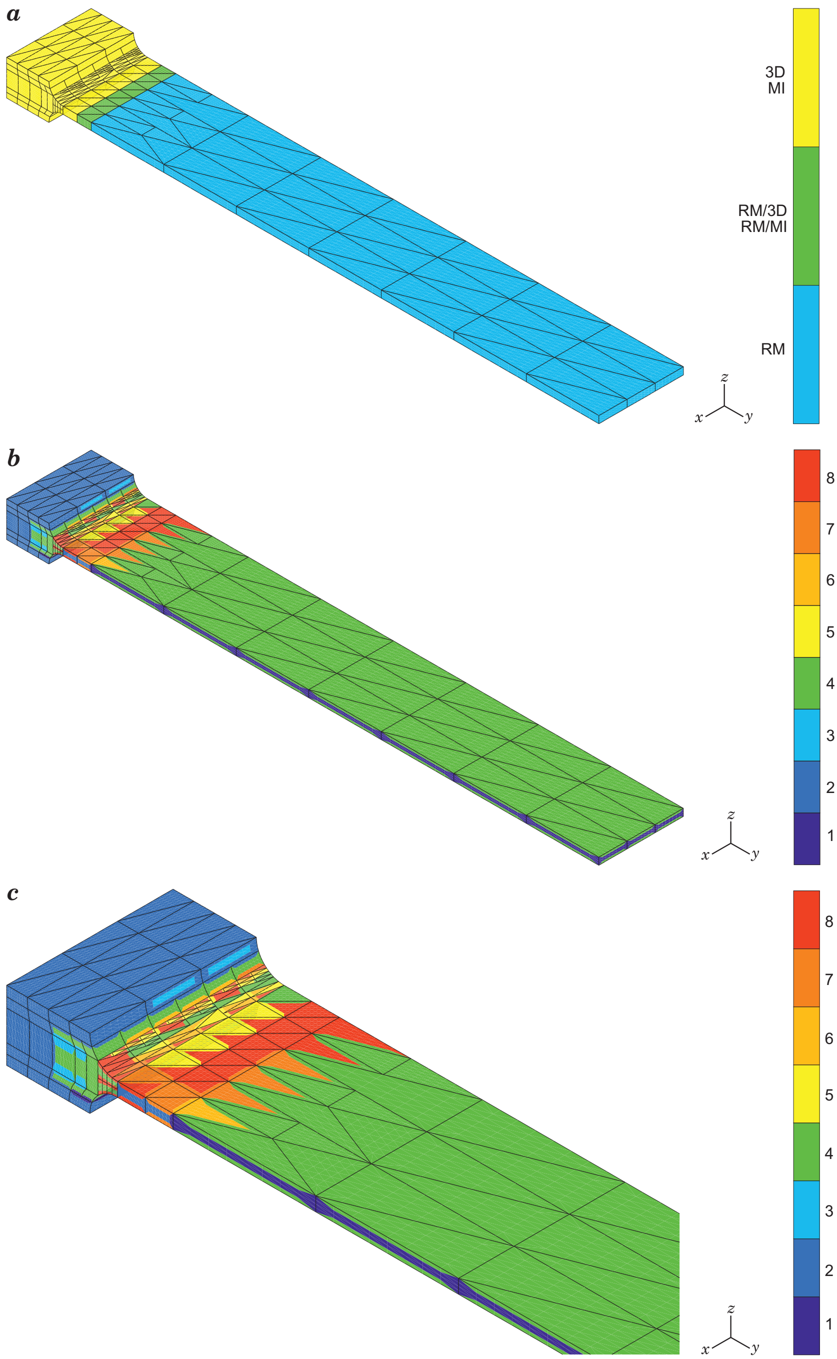

Fig. 3. Final mesh with classical transition elements: *a* – models after adaptation, *b* – orders of approximation after *hp*-adaptation, *c* – orders of approximation (enlargement)

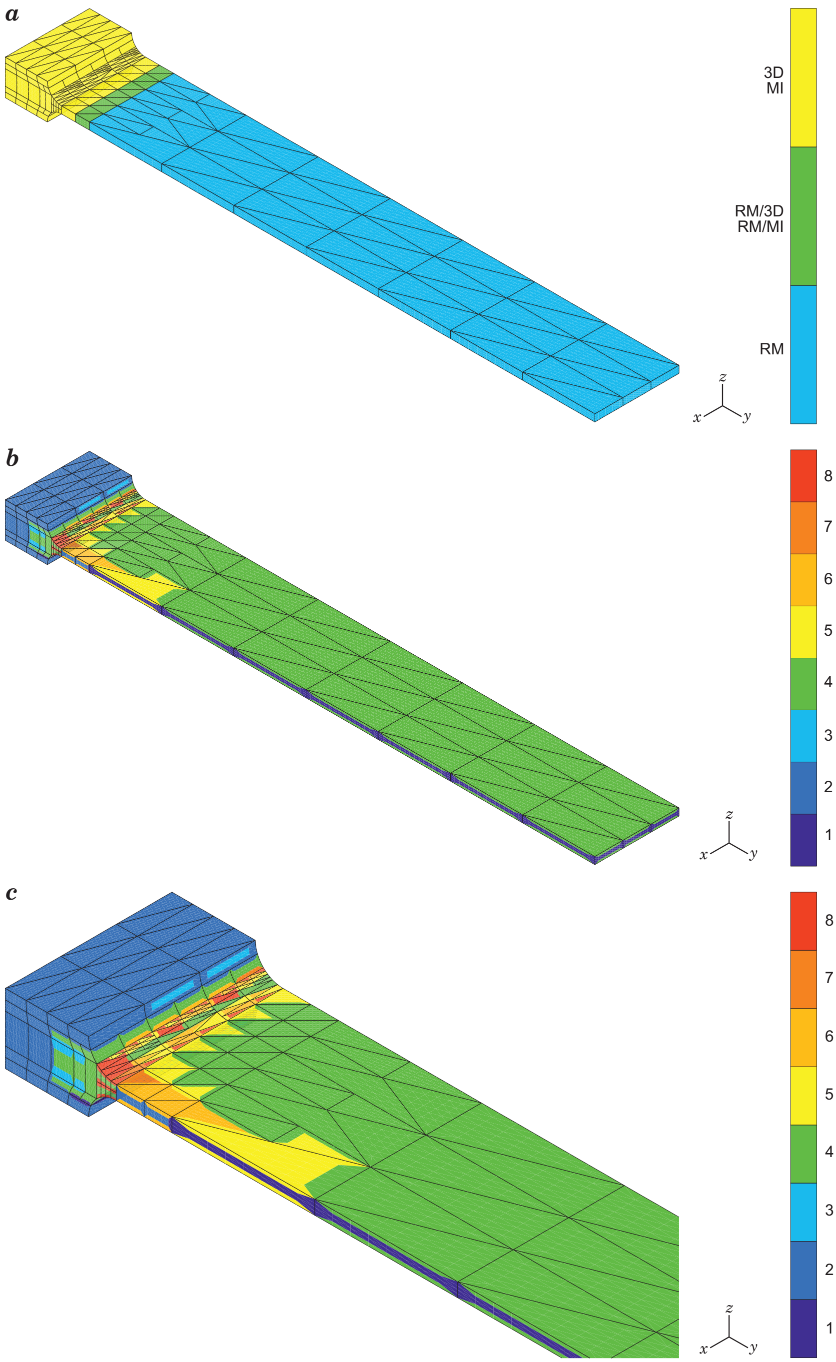

Fig. 4. Final mesh with enhanced transition elements: *a* – models after adaptation, *b* – orders of approximation after *hp*-adaptation, *c* – orders of approximation (enlargement)

In the numerical experiments, the initial mesh common for both transition models (Fig. 2) was used for the symmetric half of the blade. The first-order shell (RM), solid-to-shell transition (RM/3D), and three-dimensional (3D) models are employed in the complex blade models. The directional division numbers m are $3 \times 4 \times 2$ with $p = 2$ for the top and bottom solid blocks of the base. For the solid left and right middle blocks of the base, the division numbers are $3 \times 4 \times 1$ with $p = 2$ and $3 \times 2 \times 1$ with $p = 4$, respectively. Finally, in the right (solid-to-shell) and left (shell) blocks of the airfoil, we have $3 \times 1 \times 1$ with $p = 4$, $q = 2$ (solid part) or $q = 1$ (shell part), and $3 \times 7 \times 1$ with $p = 4$, $q = 1$, respectively. In the adaptation, the possible three-dimensional or longitudinal orders of approximation are $p = 1, 2, \ldots, 8$ in all geometrical blocks of the mesh. The possible transverse orders of approximation within shell blocks and shell parts of the solid-to-shell blocks are $q = 1, 2, \ldots, 8$ in each such block. The possible directional division numbers within geometrical blocks are $m = 1, 2, \ldots, 8$.

The corresponding final meshes are presented in Figures 3 and 4 for the models employing classical and enhanced transition models, respectively. Both were obtained as a result of the model and *hp*-adaptation process described in the next sections. The intermediate meshes can be deduced from the final meshes and the initial mesh (Fig. 2), i.e. the intermediate meshes possess division patterns of the final meshes and approximation orders of the initial mesh.

Removing the internal boundary layer

The results obtained when using two variants of transition elements are compared below. The images of effective stresses obtained using the classical (Fig. 5) and enhanced (Fig. 6) transition elements are displayed.

Both, in the case of the initial meshes (Figs. 5, 6) and the final *hp*-adapted meshes (Figs. 7, 8), the ability of the enhanced transition element to remove the internal boundary layer (between transition and first-order models) is greater than that of the classical transition element. Comparing the corresponding results from the initial and final meshes, it can be seen that in the case of richer discretization, the ability of the element to remove the internal boundary layer increases both in the case of the classical and the enhanced element. The above characteristics apply not only to the initial and final meshes but also to intermediate meshes (after step h of adaptation), not included in the illustrations. It is also worth noting that results for the modified element employed, not shown in the illustrations, look practically identical to the results obtained with the enhanced element.

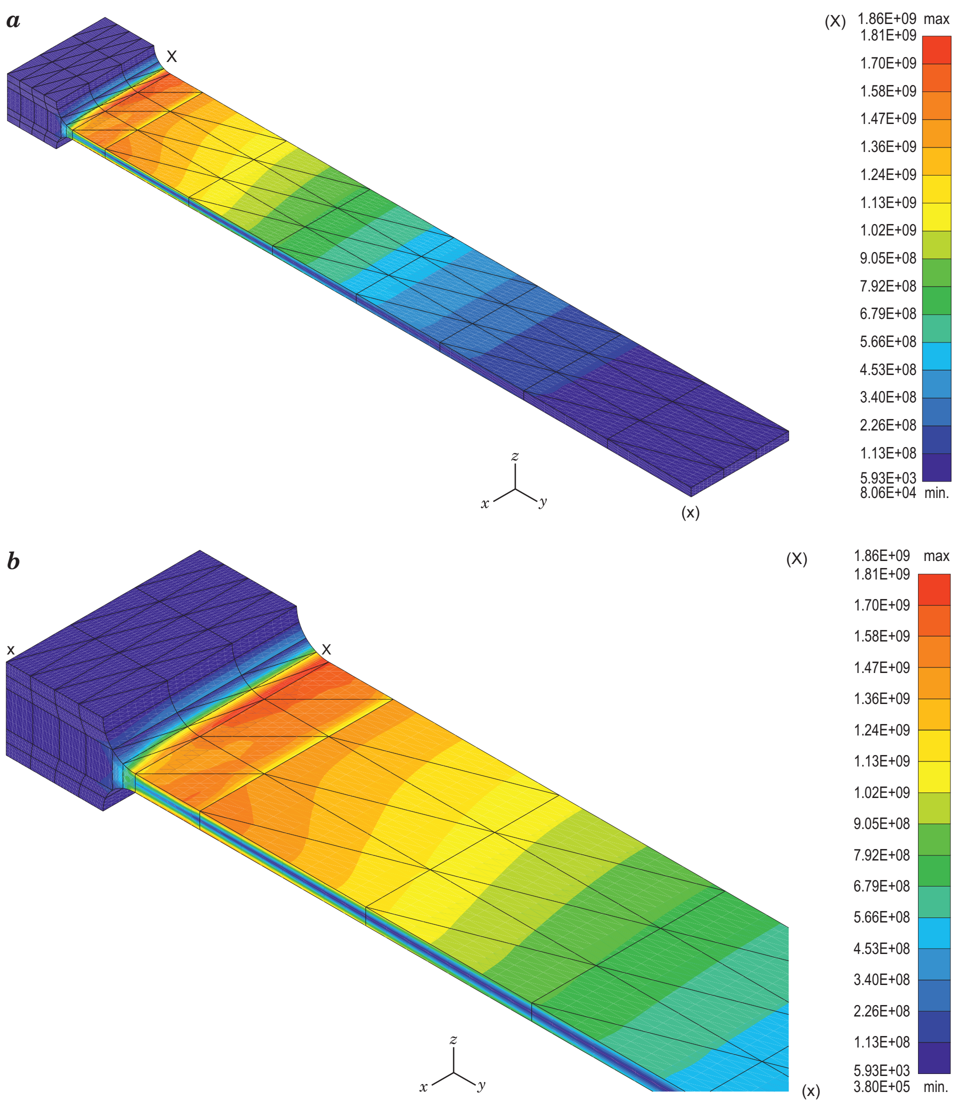

Fig. 5. Effective stresses in the initial mesh – classical transition model employed: *a* – the whole blade, *b* – enlargement of the transition zone

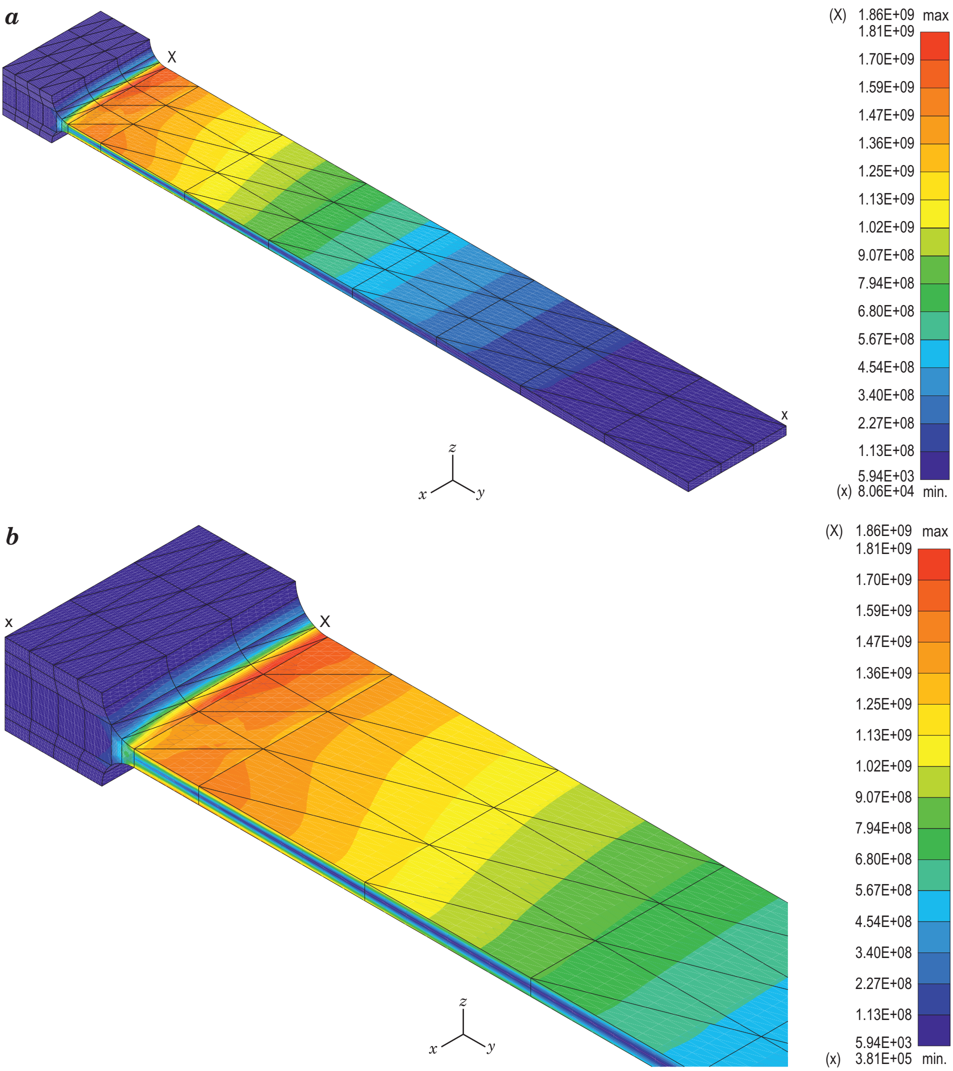

Fig. 6. Effective stresses in the initial mesh – enhanced transition model employed: *a* – the whole blade, *b* – enlargement of the transition zone

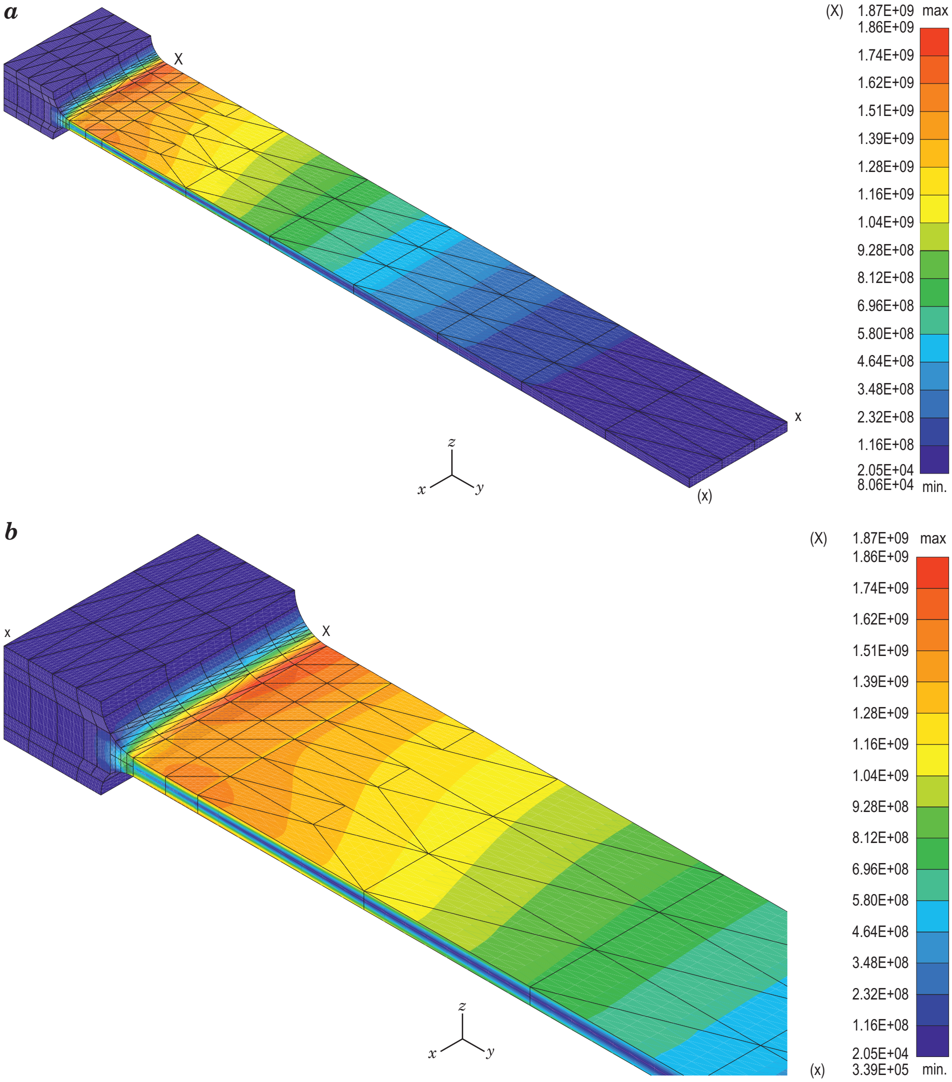

Fig. 7. Effective stresses in the final mesh – classical transition model employed: *a* – the whole blade, *b* – enlargement of the transition zone

The effectiveness of the adaptation process

The effectiveness of the adaptation process was assessed based on the results obtained in the three-step *hp*-adaptation process proposed by ODEN (1993). The method consists of solutions to the problem on the initial, intermediate, and final meshes. This approach was extended by us in ZBOIŃSKI (2013) for complex structures where shell, solid-to-shell transition, and solid parts are present.

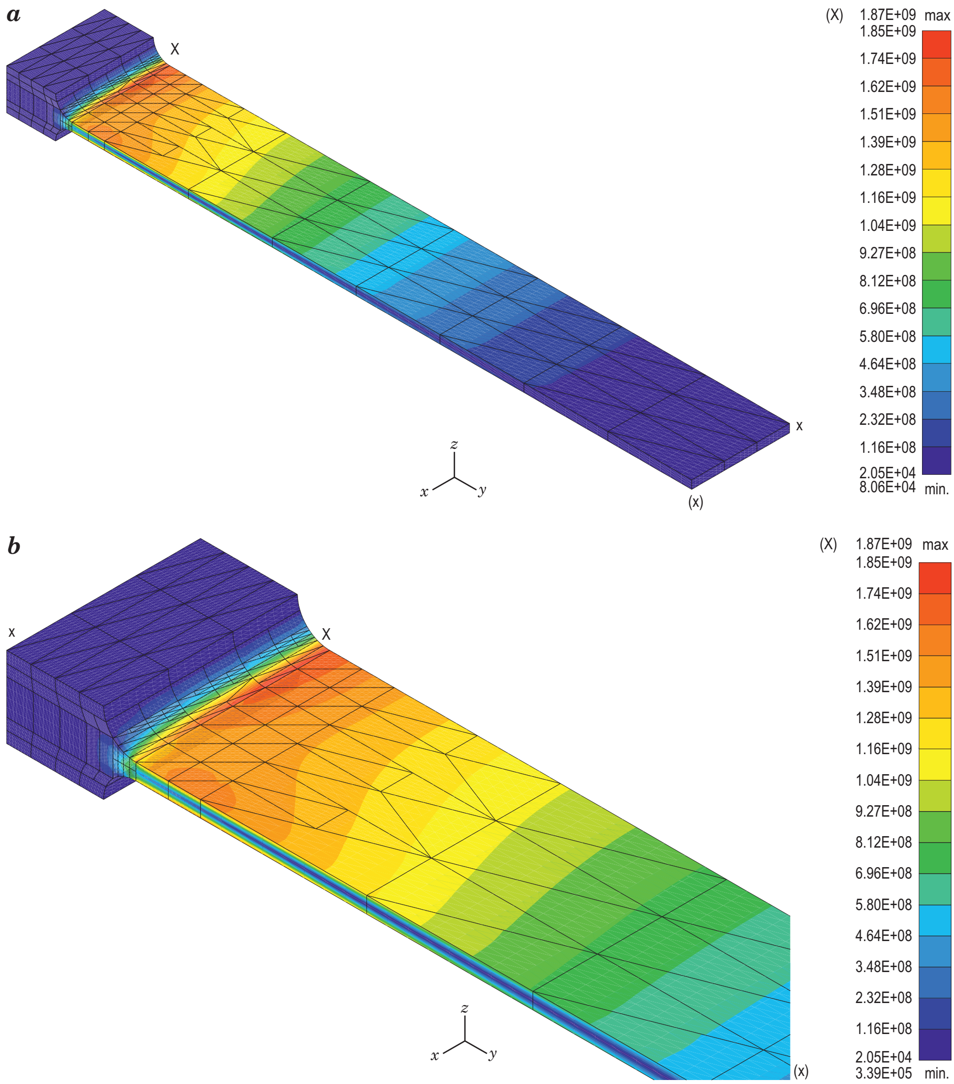

Fig. 8. Effective stresses in the final mesh – enhanced transition model employed:
a – the whole blade, *b* – enlargement of the transition zone

The three-step strategy is presented in Figure 9. The estimated error values controlling the adaptation are obtained from the equilibrated residual method (ERM) originally proposed by AINSWORTH and ODEN (1992) and adopted for the hierarchical models by ODEN and CHO (1996) and ZBOIŃSKI (2013). Our extended approach allows for different size h, and longitudinal q and transverse p orders of approximation in each finite element. This needs to relate ERM estimated error

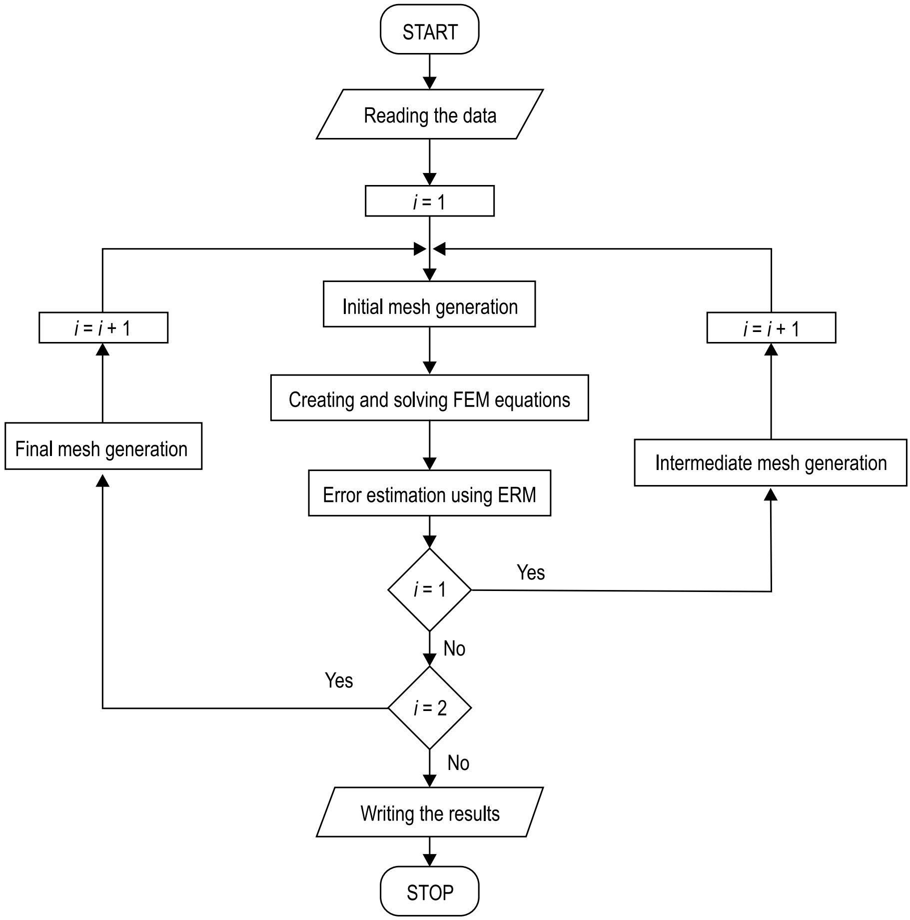

Fig. 9. The block diagram of the algorithm

values with the discretization parameters h, p and q via convergence theories. The details of the algorithm can be found in ZBOIŃSKI (2013).

The assumed value of global approximation error in the final mesh was $\gamma_T = 0.03$, while the ratio of the estimated error values in the intermediate mesh (after step h) and the final mesh (after step p) was equal to $\gamma_I/\gamma_T = 2.0$.

Figure 10 compares the estimated values of approximation errors that control the adaptation processes starting with the identical initial meshes from Figure 2 and corresponding to the introduction of either classical or enhanced transition elements to the model. It can be seen that the highest relative error values obtained from ERM are located at the airfoil-base joint where the highest strain and stress gradients appear due to the highest bending moments. This results in the densest mesh and the highest p-orders in this zone. The adaptation process and error estimation were carried out following the work already mentioned

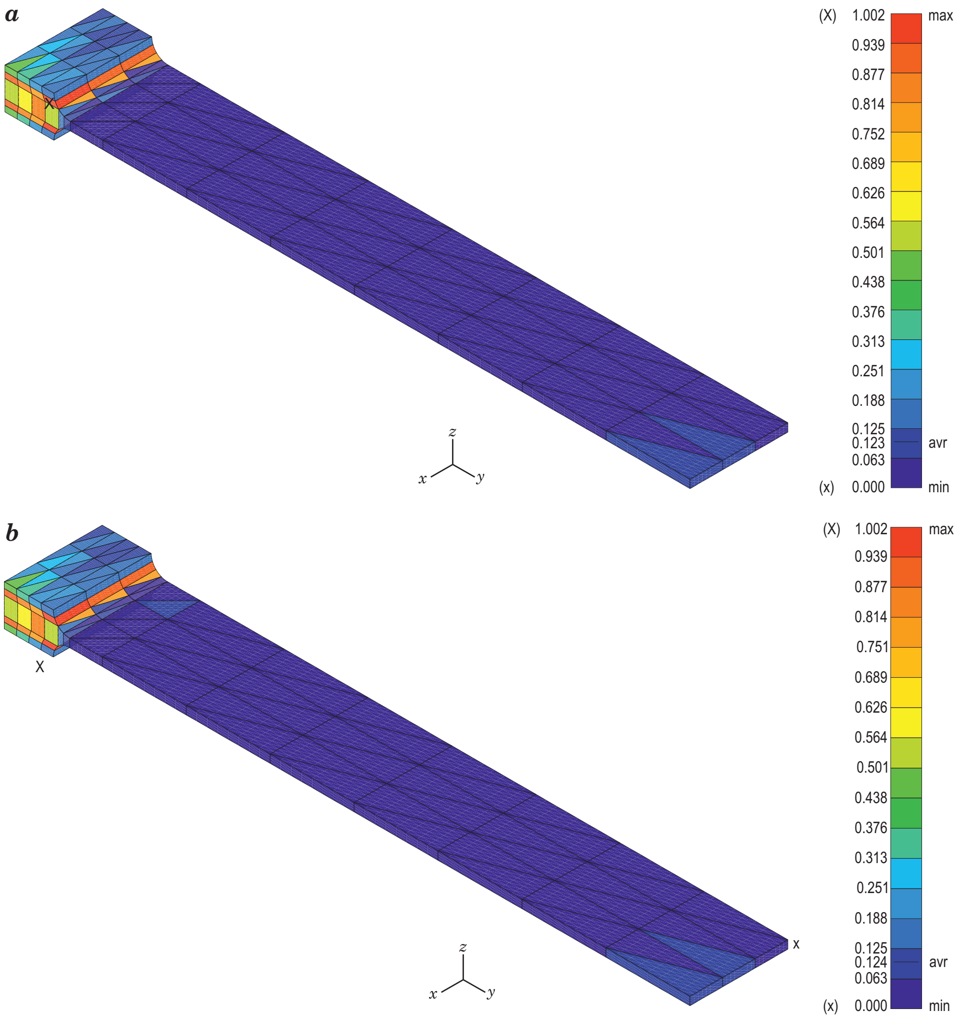

Fig. 10. Distribution of estimated values of element approximation errors – initial mesh: *a* – classical transition model, *b* – enhanced transition model

(ZBOIŃSKI 2013) which includes classical transition elements only. In the present work, we used the same approach for the modified and enhanced transition elements.

An almost identical level of element and global approximation error estimates is visible. The relative estimated global error (average) when taking into account the classical element is equal to *avr* = 0.123. In the case of the enhanced transition element, this error is equal to *avr* = 0.124. The similarity of error distributions results in almost identical intermediate meshes (not shown in the figures) and similar final meshes (Figs. 3, 4).

The estimated values of the same error in the case of different final meshes shown in Figures 3 and 4, using the classical and enhanced transition elements, respectively, are illustrated in Figure 11. The estimated values of the local and global approximation error are similar in both cases. The global (average) values are equal respectively to *avr* = 0.106 and *avr* = 0.107.

The automatic adaptation process discussed above can be also characterized by the adaptation convergence curves (Fig. 12) which relate the true relative strain energy error $(U_R - U)/U_R$ with the global number N of degrees of freedom in the mesh, with U_R and U representing strain energies of the numerical solution

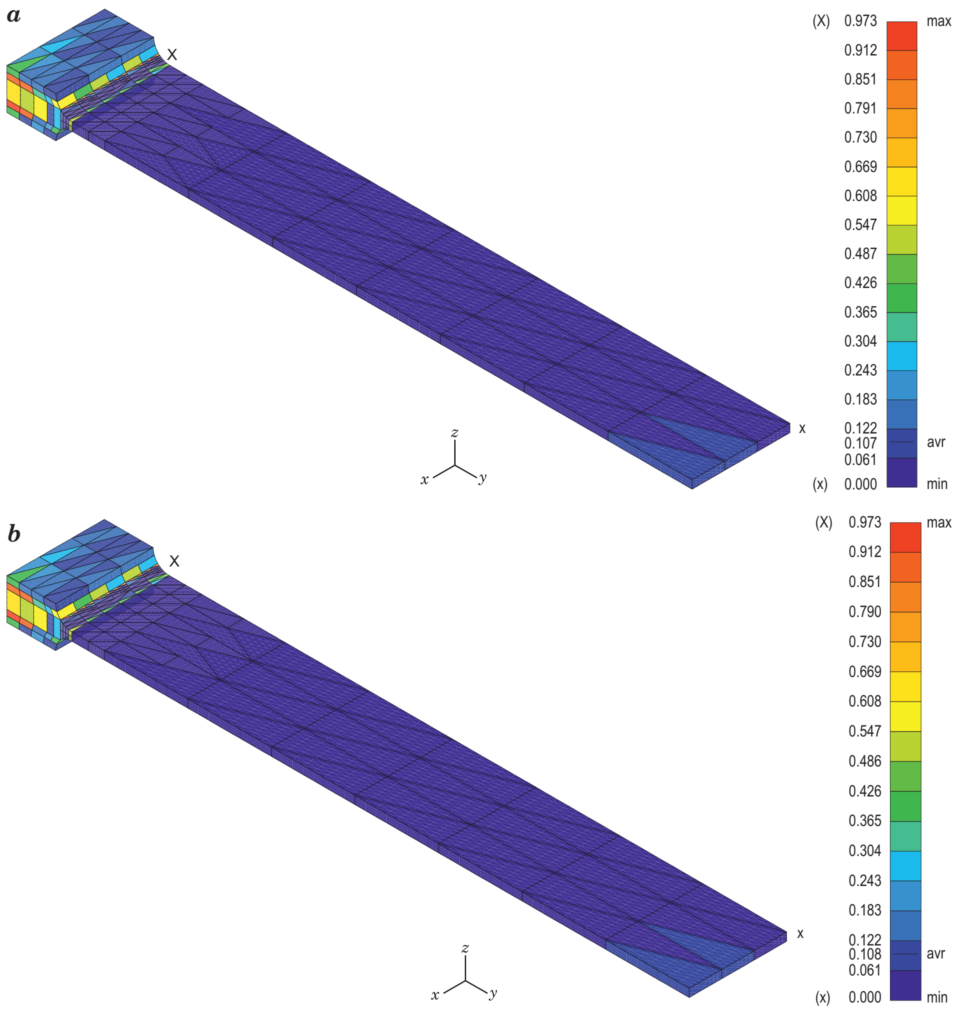

Fig. 11. Distribution of estimated values of element approximation errors – final mesh: *a* – classical transition model, *b* – enhanced transition model

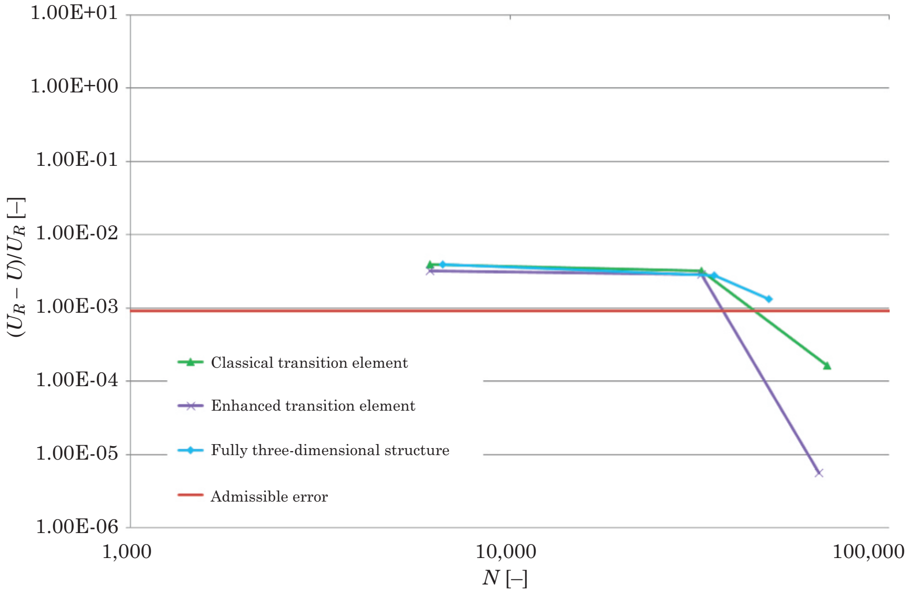

Fig. 12. Convergence curves of the three-step adaptation process

and the exact or reference solution (here approximated by the results from the richest mesh possible). For the reference solution, the directional division numbers m were $3 \times 4 \times 2$ with $p = 8$ for the top and bottom solid blocks of the base. For the solid left and right middle blocks of the base, the division numbers were $3 \times 4 \times 1$ with $p = 8$ and $3 \times 2 \times 1$ with $p = 9$, respectively. Finally, in the right (solid-to-shell) and left (shell) blocks of the airfoil, we used $3 \times 1 \times 1$ with $p = 9$, $q = 2$ (solid part) or $q = 1$ (shell part) and $3 \times 7 \times 1$ with $p = 9$, $q = 1$, respectively. The first point of the presented curves corresponds to the initial meshes, while the second and third points refer to the intermediate and final meshes. Thus, one obtains a typical picture of the error-controlled *hp*-adaptation curves where three meshes and their errors and two adaptation steps, i.e. *h* (from the initial to intermediate mesh) and *p* (from the intermediate to final mesh) are present. This reflects the main advantage of the applied adaptation strategy, i.e. its ability to obtain numerical solutions of assumed accuracy in two adaptation steps only. The assumed admissible error line corresponds to $(U_R - U)/\ U_R = (\gamma_T)^2$.

It can be seen that the *h*-adaptation delivers a similar order of convergence for models with the classical and enhanced transition models. However, in the case of step *p*, the enhanced model is more effective in diminishing the error than the classical model. Due to the almost identical discretization patterns (similar division into elements and similar orders of approximation), the effect of a greater reduction in the true approximation error in the case of the enhanced model can be attributed to the greater efficiency of this model than of the classical model.

Referring to the effectiveness of the adaptation process, it should be noted that Figure 12 also contains a third curve (blue) corresponding to the solution of a fully three-dimensional problem. This curve shows a convergence similar to that of complex models including transition elements at step h. However, at step p the convergence is lower than that of complex models. This is because the fully three-dimensional (3D) structure has, in the thin-walled part (blade airfoil), hierarchical-shell elements that tend to generate an external boundary layer. Achieving higher convergence for this model would therefore require removing the consequences of this phenomenon by introducing an exponentially denser mesh at the edges of the blade. On the contrary, in the case of the complex blade models, the blade airfoil is modeled using the first-order shell model, which is characterized by no tendency to generate an external boundary layer. Hence the higher convergence of the adaptation process in the case of complex blade models.

In order to further demonstrate the effectiveness of the applied adaptation method, the h- and p-convergence curves for enforced block-wise uniform longitudinal h-refinement of the initial mesh and block-wise three-dimensional or longitudinal p-enrichment within this mesh, are presented in Figure 13 with the use of the classical and enhanced transition elements. The points of h-convergence curves corresponded to m equal to $1 \times 2 \times 1$, $2 \times 3 \times 1$, $3 \times 4 \times 2$, $4 \times 5 \times 3$, $5 \times 6 \times 4$, $6 \times 7 \times 5$, $7 \times 8 \times 6$, $8 \times 8 \times 7$ for the top and bottom solid blocks of the base. For the left and right middle blocks of the base, the division numbers

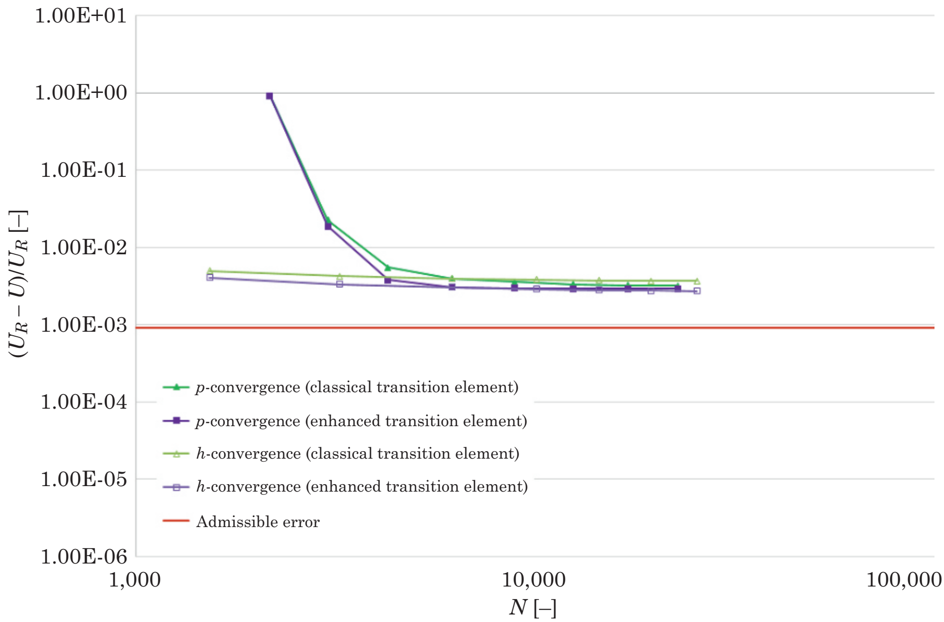

Fig. 13. Block-wise uniform h- and p-convergence curves

were 1 × 2 × 1, 2 × 3 × 1, 3 × 4 × 1, 4 × 5 × 1, 5 × 6 × 1, 6 × 7 × 1, 7 × 8 × 1, 8 × 8 × 1 and 1 × 1 × 1, 2 × 1 × 1, 3 × 2 × 1, 4 × 3 × 1, 5 × 4 × 1, 6 × 5 × 1, 7 × 6 × 1, 8 × 7 × 1, respectively. Finally, in the right (solid-to-shell) and left (shell) blocks of the airfoil, we had 1 × 1 × 1, 2 × 1 × 1, 3 × 1 × 1, 4 × 1 × 1, 5 × 1 × 1, 6 × 1 × 1, 7 × 1 × 1, 8 × 1 × 1 or 1 × 5 × 1, 2 × 6 × 1, 3 × 7 × 1, 4 × 8 × 1, 5 × 8 × 1, 6 × 8 × 1, 7 × 8 × 1, 8 × 8 × 1, respectively. These curves were obtained with the approximation orders p and q taken from the initial mesh in each block. The points of the p-convergence curves were obtained for the changing three-dimensional or longitudinal values of p with the transverse order q and division numbers m as for the initial mesh in each block. The values of p were: 1, 2, 3, 4, 5, 6 for the top, bottom and middle left solid blocks of the base, 3, 4, 5, 6, 7, 8 for the right middle (solid) block of the base, and the right (solid-to-shell) and left (shell) blocks of the airfoil. The h- and p-convergence curves corresponding to classical and enhanced elements cross at the first (initial) points of the adaptive convergence curves from Figure 12. Exponential convergence of the p-curves, typical for some model problems, is not observed due to combined convergence presented in the figure, corresponding to different convergence rates in solid, solid-to-shell and shell parts of the blade. Hence, also combined hp-convergence (not presented), obtained from enforced block-wise uniform meshes, is not expected to be exponential. Comparing the h- and p-curves with the hp-adaptation convergence curves one can conclude that the admissible error value was reached only in the case of automatic hp-adaptation with the use of the complex blade models only. Additionally, the adapted meshes need much fewer degrees of freedom than the uniform meshes to obtain the same error level.

Conclusions

It was demonstrated that the modified and enhanced transition elements employed for modeling complex models of real technical objects, e.g. turbine blades, possess a greater ability to remove the internal boundary layer between the transition and first-order shell model than the classical transition model.

It was also shown that the enhanced transition elements employed in complex structures deliver the highest adaptive convergence of the solutions to complex models of the blade or other technical objects.

Considering the effectiveness of the adaptation process of the complex model of the rotor turbine blade (or other structures), it should be noted that obtaining the same level of errors from the basic model of three-dimensional elasticity and the complex models employing transition elements requires a smaller number of degrees of freedom in the latter case. This perfectly justifies the use of complex models instead of the basic model of three-dimensional elasticity, if only the approximation error is taken into consideration.

References

AINSWORTH M., ODEN J.T. 1992. *A procedure for a posteriori error estimation for h-p finite element methods*. Computer Methods in Applied Mechanics and Engineering, 101: 73-96.

COFER W.F., WILL K.M. 1991. *A Three-dimensional, Shell-solid transition element for general nonlinear analysis*. Computers & Structures, 38: 449-462.

DÁVILA C.G.1994. *Solid-to-shell transition elements for the computation of interlaminar stresses*. Computing Systems in Engineering, 5: 193-202.

DEMKOWICZ L. 2006. *Computing with hp-Adaptive Finite Elements*. Volume I. *One and Two--Dimensional Elliptic and Maxwell Problems*. Chapman &Hall/CRC Press, Taylor and Francis Group, Boca Raton.

GMÜR T.C., SCHORDERET A.M. 1993. *A set of three-dimensional solid to shell transition elements for structural dynamics*. Computers & Structures, 46: 583-591.

HUANG F., XIE X. 2011. *A Modified Nonconforming 5-Node Quadrilateral Transition Finite Element*. Advances in Applied Mathematics and Mechanics, 2: 784-797.

JEYACHANDRABOSE C., KIRKHOPE J. 1984. *Construction of transition finite elements for the plane triangular family*. Computers & Structures, 18: 1127-1134.

NOSARZEWSKA M. 2007. *Zastosowanie elementów przejściowych w adaptacyjnej analizie struktur sprężystych*. Praca magisterska. Wydział Nauk Technicznych, Uniwersytet Warmińsko--Mazurski, Olsztyn.

NOSARZEWSKA M., ZBOIŃSKI G. 2009. *Efektywność przejściowych elementów skończonych w hierarchicznym modelowaniu struktur złożonych*. Modelowane Inżynierskie, 7(38): 131-138.

ODEN J.T. 1993. *Error estimation and control in computational fluid dynamics. The O.C. Zienkiewicz Lecture*. Proc. Math. of Finite Elements - MAFELAP VIII, 1-36. Brunnel Univ., Uxbridge.

ODEN J.T, CHO J.R. 1996. *Adaptive hpq-finite element methods of hierarchical models for plate- and shell-like structures*. Computer Methods in Applied Mechanics and Engineering, 136: 317-345.

RANK E., BABUŠKA I. 1987. *An expert system for the optimal mesh design in the hp-version of the finite element method*. International Journal for Numerical Methods in Engineering, 24: 2087-2106.

SCHWAB C. 1998. *p and hp FEM*. Oxford University Press, Oxford.

SURANA K.S. 1980. *Transition finite elements for three-dimensional stress analysis*. International Journal for Numerical Methods in Engineering, 15: 991-1020.

SURANA K.S. 1982. *Geometrically non-linear formulation for the three dimensional solid-shell transition finite elements*. Computers & Structures, 15: 549-566.

SURANA K.S. 1983. *Geometrically nonlinear formulation for the axi-simetric transition finite element*. Computers & Structures, 17: 243-255.

SURANA K.S. 1987. *Three dimensional solid-shell transition finite elements for heat conduction*. Computers & Structures, 26: 941-950.

SZABÓ B.A., SAHRMANN G.J. 1998, *Hierarchic plate and shell models based on p-extension*. International Journal for Numerical Methods in Engineering, 26: 1855-1881.

WAN K.H. 2004. *Transition finite elements for mesh refinement in plane and plate Bendig analyses*. MSc Thesis. Mechanical Engineering Department, The University of Hong Kong.

ZBOIŃSKI G. 1997. *Application of the three-dimensional triangular-prism hpq adaptive finite element to plate shell analysis*. Computers and Structures, 65(4): 497-514.

ZBOIŃSKI G. 2001. *Modelowanie hierarchiczne i metoda elementów skończonych do adaptacyjnej analizy struktur złożonych*. Zeszyty Naukowe IMP PAN w Gdańsku. Studia i Materiały. Instytut Maszyn Przepływowych PAN, Gdańsk.

ZBOIŃSKI G. 2010. *Adaptive hpq finite element methods for the analysis of 3D-based models of complex structures*. Part 1. *Hierarchical modeling and approximation*. Computer Methods in Applied Mechanics and Engineering, 199: 2913-2940.

ZBOIŃSKI G. 2013. *Adaptive hpq finite element methods for the analysis of 3D-based models of complex structures*. Part 2. *A posteriori error estimation*. Computer Methods in Applied Mechanics and Engineering, 267: 531-565.

ZBOIŃSKI G., JASIŃSKI M. 2007. *3D-based hp-adaptive first-order shell finite element for modelling and analysis of complex structures*. Part 1. *The model and the approximation*. International Journal for Numerical Methods in Engineering, 70: 1513-1545.

ZBOIŃSKI G., OSTACHOWICZ W. 2000. *An algorithm of a family of 3D-based, solid-to-shell, hpq/hp-adaptive finite elements*. Journal of Theoretical and Applied Mechanics, 38: 791-806.

ZIELIŃSKA M., ZBOIŃSKI G. 2013. *Opracowanie efektywnego numerycznie sformułowania adaptacyjnego, opartego na podejściu trójwymiarowym, bryłowo-powłokowego elementu przejściowego zapewniającego ciągłość pola naprężeń pomiędzy modelami podstawowymi*. Raport wewnętrzny, nr arch. 324/15, Instytut Maszyn Przepływowych PAN, Gdańsk.

ZIELIŃSKA M., ZBOIŃSKI G. 2014a. *Analiza płyt i powłok zdominowanych membranowo z ciągłą zmianą naprężeń i odkształceń w strefach przejściowych*. Mechanik, 87: 855-872.

ZIELIŃSKA M., ZBOIŃSKI G. 2014b. *hp-Adaptive finite element analysis of thin-walled structures with use of the shell-to-shell transition elements*. In: *Recent Advances in Computational Mechanics*. Eds. T. Lodygowski, J. Rakowski, P, Litewka. CRC Press, London.